Accepted Manuscript

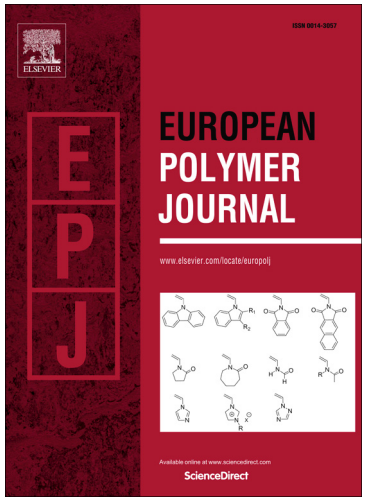

HYBRID NANOCOMPOSITES OF THERMOPLASTIC ELASTOMER AND CARBON NANOADDITIVES FOR ELECTROMAGNETIC SHIELDING

Scheyla Kuester, Nicole R. Demarquette, José Carlos Ferreira Jr., Bluma G. Soares, Guilherme M. O. Barra

PII: S0014-3057(16)31019-9
DOI: http://dx.doi.org/10.1016/j.eurpolymj.2017.01.023
Reference: EPJ 7684

To appear in: *European Polymer Journal*

Received Date: 28 September 2016
Revised Date: 7 January 2017
Accepted Date: 19 January 2017

Please cite this article as: Kuester, S., Demarquette, N.R., Carlos Ferreira, J. Jr., Soares, B.G., M. O. Barra, G., HYBRID NANOCOMPOSITES OF THERMOPLASTIC ELASTOMER AND CARBON NANOADDITIVES FOR ELECTROMAGNETIC SHIELDING, *European Polymer Journal* (2017), doi: http://dx.doi.org/10.1016/j.eurpolymj.2017.01.023

HYBRID NANOCOMPOSITES OF THERMOPLASTIC ELASTOMER AND CARBON NANOADDITIVES FOR ELECTROMAGNETIC SHIELDING

Scheyla Kuester[1,2], Nicole R. Demarquette[1*], José Carlos Ferreira Jr.[2], Bluma G. Soares[3], Guilherme M. O. Barra[2#]

[1*]École de technologie supérieure de Montréal, Mechanical Engineering Department, Montreal, QC, Canada
E-mail: NicoleR.Demarquette@etsmtl.ca
[2#]Universidade Federal de Santa Catarina, Departamento de Engenharia Mecânica, Florianópolis, SC, Brazil,
E-mail: g.barra@ufsc.br
[3]Universidade Federal do Rio de Janeiro, Departamento de Engenharia Metalúrgica e de Materiais, Rio de Janeiro, RJ, Brazil.

ABSTRACT

Hybrid nanocomposites of poly (styrene-b-ethylene-ran-butylene-b-styrene) (SEBS), graphene nanoplatelets (GnP), and carbon nanotubes (CNT) were successfully prepared by melt compounding for electromagnetic shielding applications. The morphologies of the carbon nanoadditives and nanocomposites were investigated by Raman spectroscopy, field emission gun scanning electron microscopy, and rheological analysis. DC electrical conductivity was assessed by two-probe and four-probe techniques. Electromagnetic interference shielding effectiveness, shielding mechanisms, and dielectric properties were conducted in the X-band microwave frequency range (8.2-12.4 GHz). The results showed that CNT had a higher affinity with the matrix, and were better dispersed than GnP. SEBS/GnP/CNT nanocomposites induced an electrical conductivity increase of 17 orders of magnitude compared to the polymer matrix. The hybrid nanocomposites presented synergic effects on EMI-SE when compared to the single-component nanocomposites (SEBS/GnP and SEBS/CNT). The maximum EMI-SE of 36.47dB (reduction of 99.98% of the incident radiation) was achieved for the SEBS/GnP/CNT nanocomposite with 5/10 wt.% of GnP/CNT, respectively. All the hybrid nanocomposites with CNT loadings equal to or higher than 8 wt.%. presented the required EMI-SE for commercial applications.

Keywords: Hybrid nanocomposites; Graphene nanoplatelets; Carbon Nanotubes; Electrical properties; Electromagnetic shielding effectiveness.

1. INTRODUCTION

The current information age has clearly brought deep changes to the human way of life, with nanotechnology increasingly incorporated into our daily routine, and modern society experiencing the phenomenon of technology miniaturization. Alongside the mostly beneficial changes that this new order has ushered in, the fast and growing proliferation of equipment and mobile electronic devices, such as cell phones, laptops, and tablets, have also given rise to serious problems of electromagnetic interferences (EMI), and possibly to human diseases. As a result, shielding materials, especially those based on polymer nanocomposites consisting of insulating polymer matrices and conductive carbon nanoparticles, are being widely studied in a bid to overcome these problems [1-8].

Carbon nanoparticles, such as carbon nanotubes (CNTs) and graphene (GR), exhibit huge specific areas, high aspect ratios, extraordinary mechanical properties, and high thermal and electrical conductivities. For EMI shielding applications, polymer nanocomposites of CNT generally exhibit high electromagnetic interference shielding effectiveness (EMI-SE). Currently, however, CNT obtained by chemical vapor deposition (CVD) are usually expensive, leading to graphene produced from graphite being used as a cheaper alternative [9]. Recently, the search for synergic effects and cost reductions led to studies of hybrid polymer nanocomposites of carbon nanoparticles [1, 6, 10-13]. According to the literature, the combination of carbon nanoadditives of different shapes improves the conductive network in hybrid nanocomposites [6, 11, 13]. Hybrid nanocomposites of polystyrene (PS), CNT and graphite nanoplates, in small portions of 2/1.5 wt.% of CNT/graphite nanoplates, respectively, prepared by in situ polymerization, presented an EMI-SE of ≈ 20.2 [10], which is the shielding effectiveness usually required for commercial applications [1, 8, 10-12, 14, 15]. In another study, hybrid nanocomposites of acrylonitrile butadiene styrene (ABS), CNT, and GR, prepared by dry tumble mixing followed by hot compaction, exhibited an improvement in the EMI-SE from 7.5 to 26.8 dB by the addition of 1 wt.% of CNT to an ABS/GR nanocomposite [6]. On the other hand, ABS/CNT/Carbon black (CB) hybrid nanocomposites, prepared by solution casting followed by hot compression, did not present any synergic effects. However, the authors showed that small quantities of CNT could be replaced by CB, thereby decreasing the final cost of the nanocomposites, without impairing the EMI-SE [11].

For commercial applications of polymer composites as EMI shielding materials, the dispersion of the conductive additives is one of the most critical factors. Nevertheless, it is well known from the literature that carbon nanoparticles are very difficult to disperse in polymer matrices. Among the different compounding methods, the solvent casting technique generally provides better dispersion, while the composites produced exhibit higher EMI-SE. However, solution casting is generally not suitable for commercial applications due to its extensive use of organic solvents, as well as to the fact that the method is not environmentally friendly. For these reasons, melt compounding is a preferred method [13], and because of that, the choice of the polymer matrix plays an important role.

Poly (styrene-b-ethylene-ran-butylene-b-styrene) (SEBS) is a thermoplastic elastomer, which exhibits the properties of an elastomer, and at the same time, has the advantage of being processed as a thermoplastic material. SEBS is basically a styrenic block copolymer comprised of three interconnected blocks, two rigid (polystyrene) in the ends, and the other, rubbery (poly (ethylene-butylene)) in the middle [16-21]. Therefore, another advantage it presents relates to the fact that in systems composed of styrenic materials and carbonaceous fillers, an affinity is expected between the π electrons of both components, once their molecular structures comprise aromatic rings. These non-covalent π-π interactions may help to improve the dispersion of carbon nanoparticles inside the matrix [22-27] and enhance the EMI-SE of the final nanocomposites [1, 10, 28].

In a previous work, we studied nanocomposites of SEBS/CNT for EMI shielding prepared by melt compounding. With 10 wt.% of CNT, we obtained the SE necessary for commercial applications, that is SE > 20 dB (reduction of 99.00% of the incident radiation); with 15 wt.% of CNT, the SE was 30 dB, representing a 99.9% reduction of the incident radiation [29]. In the present work, we prepared SEBS/GnP nanocomposites and hybrid nanocomposites of SEBS/GnP/CNT via the same compounding method. The nanocomposites were characterized by

morphology, dispersion, polymer/carbon nanoparticle interactions, electrical conductivity, dielectric properties, and EMI shielding. Nanocomposites of SEBS/CNT were also prepared in order to characterize the differences between the dispersion of the different carbon nanoadditives in the SEBS polymer matrix.

2. EXPERIMENTAL

Graphene nanoplatelets (GnP), (xGnP-M-25, surface area = 120 – 150 $m^2.g^{-1}$; bulk density = 0.03 – 0.1 $g.cm^{-3}$; carbon purity = 99.5%; average particle diameter = 25 μm; particle thickness = 6 – 8 nm), was purchased from XG Sciences, Inc. Multiwalled Carbon Nanotube (MWCNT) (Nanocyl™ NC 7000 series, surface area = 250 - 300 $m^2.g^{-1}$; density bulk = 0.06 $g.cm^{-3}$; carbon purity = 90 %; average diameter = 9.5 nm; average length = 1.5 μm), was obtained from Nanocyl S.A. Poly (styrene-b-ethylene-ran-butylene-b-styrene) (SEBS) (Kraton G-1650; number-average molecular weight = 94,000 $g.mol^{-1}$; polystyrene content = 30 wt.%, bulk density = 0.224 $g.cm^{-3}$, specific gravity = 0.91 $g.cm^{-3}$) was supplied by Kraton Polymers do Brasil Ind. Com. Prod. Petr. Ltda. All materials were used as received.

Polymer nanocomposites of SEBS/GnP and SEBS/GnP/CNT were obtained by melt compounding using a torque rheometer (Haake Rheocord), which was coupled to a mixing chamber (Rheomix 600p) equipped with roller rotors. The processing parameters were set as follows: temperature of 230 °C, rotational speed of 150 rpm, and total mixing time of 25 minutes. The compression molding was performed in a hydraulic press at a temperature of 230 °C, for a total of 10 minutes at a pressing pressure of approximately 20 MPa.

The morphology of the carbon nanoparticles was characterized by field emission gun scanning electron microscopy (FEG-SEM) using a JEOL JSM-6701 F field instrument at an acceleration voltage of 10 kV. For cross-sectional analysis of the nanocomposites, samples were cryogenically fractured in liquid nitrogen and placed in an aluminum sample holder containing a double-sided conductive carbon adhesive tape, and coated with gold.

Rheological measurements (Small Amplitude Oscillatory Shear analysis (SAOS)) were performed in a MCR 501 Anton Paar rheometer equipped with plate-plate geometry. The tests were performed in the linear viscoelastic regime, at the frequency range from 0.01 to 300 $rad.s^{-1}$, and temperature of 230 °C.

The structural morphology of the carbon nanoparticles as-received and in the nanocomposites after processing was evaluated by Raman spectroscopy in a CRM (Confocal Raman Microscope) Alpha 300R Witec system with a 532nm laser excitation <100mW and a UHTS 300 (ultra-high throughput spectrometer), and gratings of 600 or 1800 g/mm, with a 500 blaze.

The DC electrical conductivity of the SEBS and nanocomposites was characterized at room temperature by the two-probe and four-probe methods, depending on the electrical conductivity of the sample. For neat SEBS and nanocomposites of low electrical conductivity, measurements were performed using the two-probe standard method, with a Keithley 6517A electrometer connected to a Keithley 8009 test fixture. For nanocomposites of higher electrical conductivity, measures were done using the four-probe standard method, with a Keithley 6220 current source to apply the current and a Keithley 6517A electrometer to measure the difference of potential. The data presented are the average of five measurements.

The EMI-SE measurements and the dielectric analysis of the nanocomposites in the X-band microwave frequency range (8.2-12.4 GHz) were performed using a microwave network analyzer (N5230C Agilent PNA-L, Santa Clara, CA). The incident and transmitted waves were represented mathematically by complex scattering parameters S_{11} (or S_{22}) and S_{12} (or S_{21}), which are correlated with the reflectance and the transmittance. In this analysis, when the incident electromagnetic radiation collides with a shielding material, the absorbance (A), reflectivity (R), and transmittance (T) totalize 1 ($T + R + A = 1$). The coefficients of absorbance (A), reflectivity (R), and transmittance (T) were obtained using S-parameters, according to equations 1 and 2 [6, 10, 14, 15, 30, 31].

$$T = [E_T/E_I]^2 = |S_{12}|^2 = |S_{21}|^2 \quad (1)$$

$$R = [E_R/E_I]^2 = |S_{11}|^2 = |S_{22}|^2 \quad (2)$$

EMI-SE measurements were carried out with an X-band waveguide as the sample holder, and the thickness of all samples was 2.0 mm.

3. RESULTS AND DISCUSSION

3.1. Morphological analysis

The morphology of GnP and CNT was studied by field emission gun scanning electron microscopy (FEG-SEM). Figure 1 presents FEG-SEM micrographs of GnP at different magnifications. As shown in Figure 1 a), b), and c), the material exhibited some agglomerations of a few layers of graphene sheets. However, from Figure 1 d), e), and f), it can be seen that the morphology was not homogeneous, and that the material also presented some agglomerates of expanded graphite sheets.

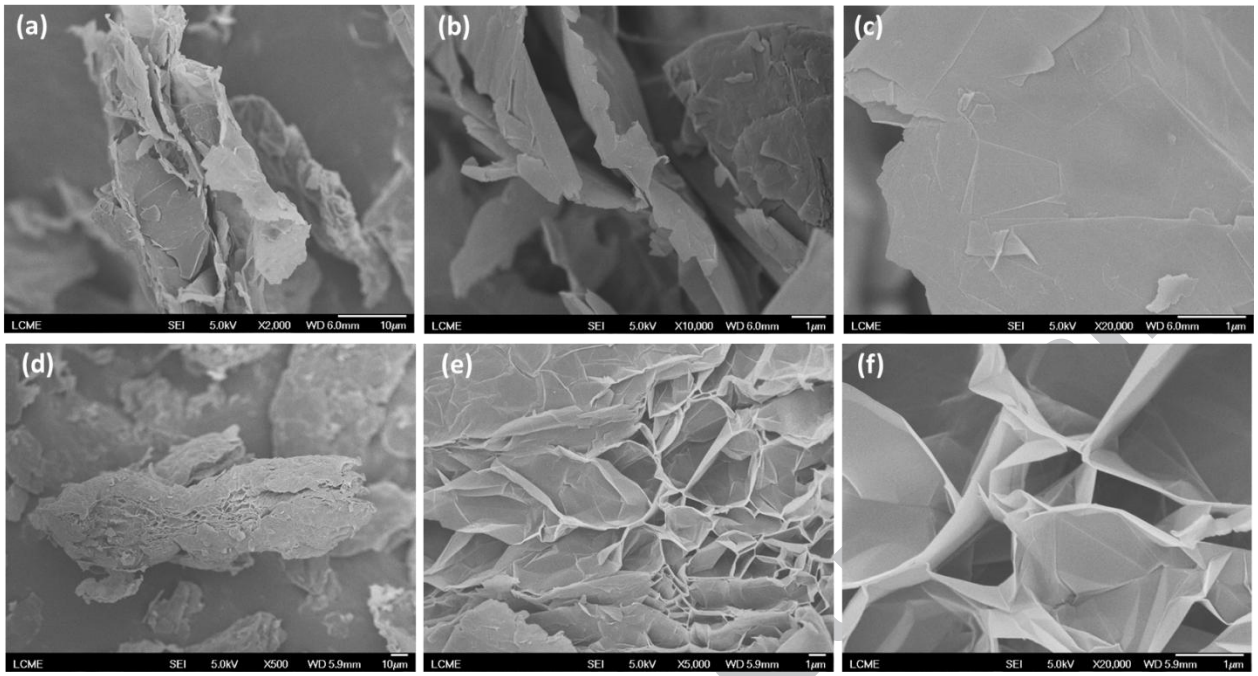

Figure 1. FEG-SEM micrographs of the as-received GnP at different regions and magnifications: a) x2000, b) x10000, c) x20000, d) x500, c) x5000, and d) x20000

Figure 2 shows the FEG-SEM micrographs of the SEBS/GnP with 10 wt.% of GnP at different magnifications. The micrograph shown in Figure 2a) indicates that GnP was uniformly distributed in the SEBS matrix. In the micrograph with a higher magnification presented in Figure 2b), it can be observed that the nanocomposite apparently exhibited decent matrix-GnP adhesion, since there is no evidence of large voids in the interface of both phases.

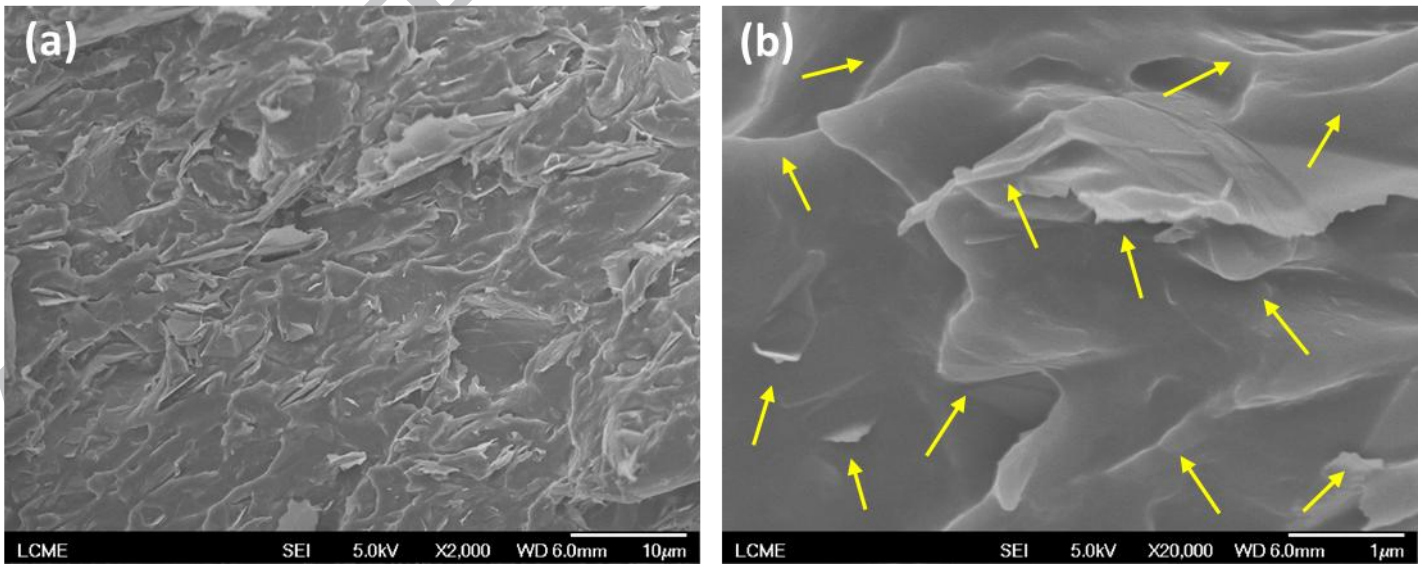

Figure 2. FEG-SEM micrographs of SEBS/GnP with 10 wt.% of GnP at different magnifications: a) x2000, b) x20000

Figure 3 shows FEG-SEM micrographs of CNT at different magnifications. The as-received CNT a) exhibited the typical structure of large agglomerates of CNT, and b) presented tubes of different diameters.

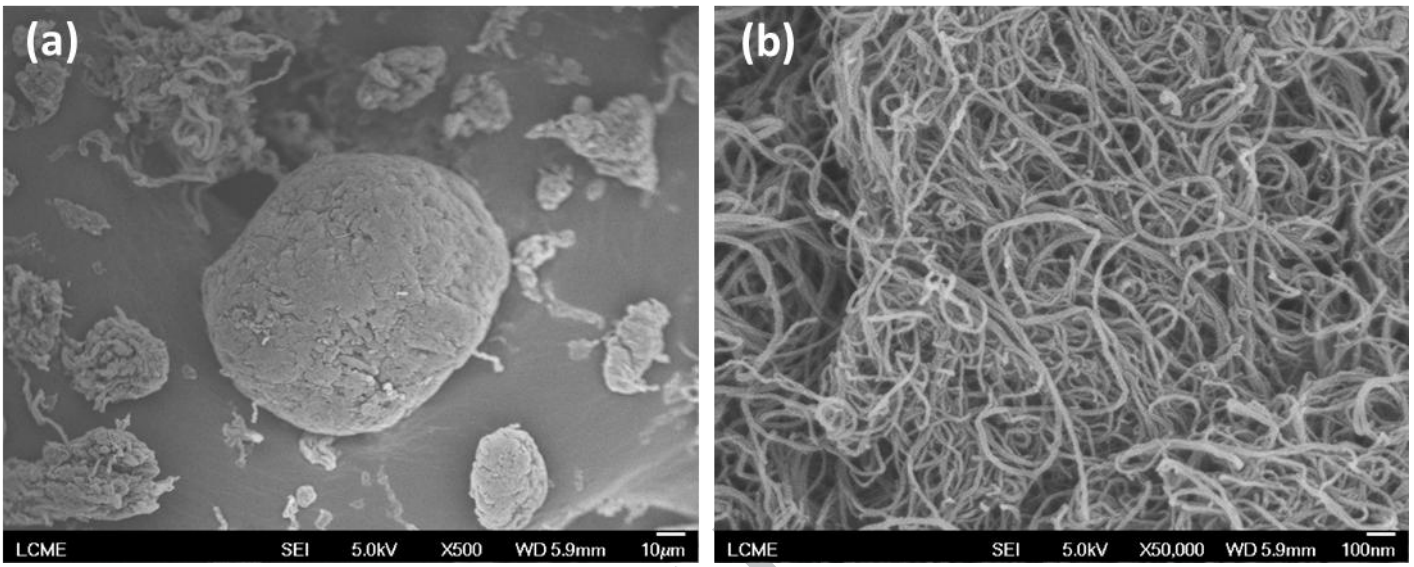

Figure 3. FEG-SEM micrographs of the as-received CNT at different magnifications: a) x500, b) x50000

Figure 4 shows the FEG-SEM micrographs of the SEBS/CNT with 10 wt.% of CNT at different magnifications.

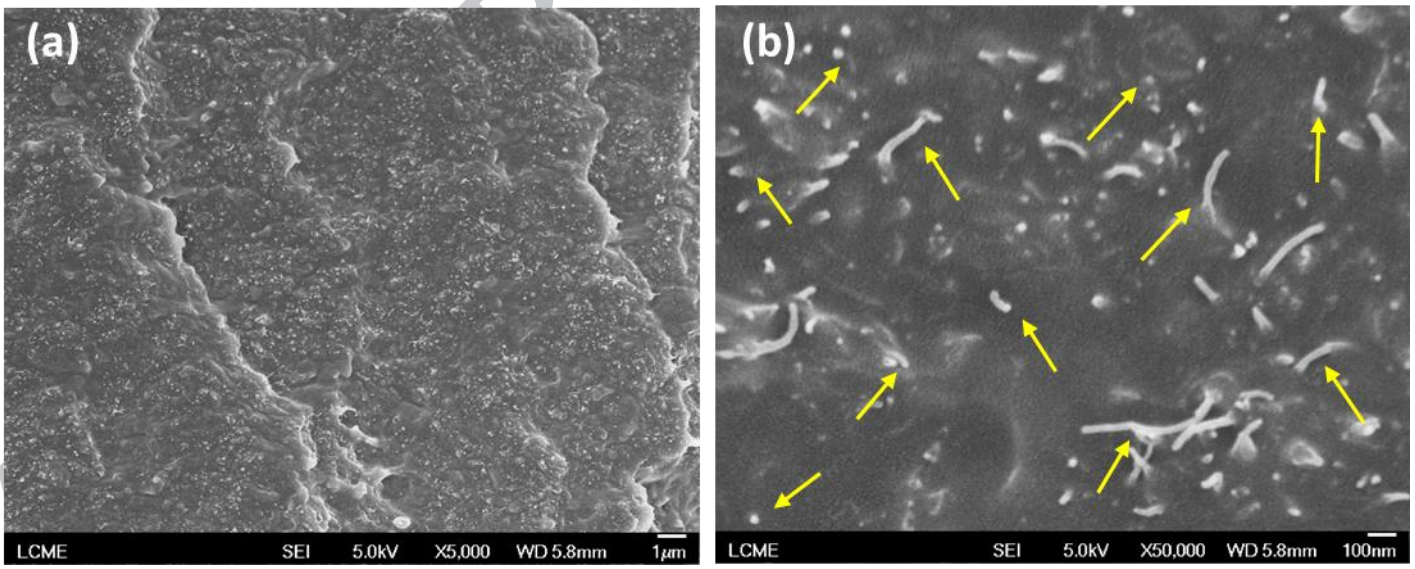

Figure 4. FEG-SEM micrographs of SEBS/CNT with 10 wt.% of CNT at different magnifications: a) x5000, b) x50000

According to the micrographs, CNT (the 4a) lighter spots) seems to be satisfactorily distributed in the SEBS matrix. In figure 4b), the image of the individualized tubes suggests that the CNT agglomerates were properly disaggregated through the melt compounding process.

The dispersion of the carbon nanoparticles through the SEBS matrix, as well as the morphological structure of SEBS, were studied by rheological analysis. In the linear viscoelastic regime, small amplitude oscillatory shear (SAOS) analysis is very useful for identifying the different possible morphologies of SEBS (such as lamellar, cylindrical, spherical, or even disordered, depending on the fraction of each block in the copolymer, and on the thermodynamic interactions between the phases). Curves of log G' vs. log ω (G' = storage modulus, ω = frequency) present different slopes in the low frequency region, corresponding to differences in the relaxation times of the phase domains; these can be used to characterize the degree of the spatial order, and consequently, the SEBS morphological structure [32]. Moreover, the study of the rheological behavior of polymer nanocomposites is also an efficient method for characterizing the dispersion of the nanoparticle into the polymeric matrix [32, 33]. By SAOS analysis, the influence of the addition of carbon nanoadditives on G' curves is studied via the evaluation of changes in the low frequency slope of log G' vs. log ω curves upon variation of carbon nanoadditives loading. Figure 5 shows the rheological behavior (SAOS) of neat SEBS and SEBS/GnP nanocomposites at low frequencies.

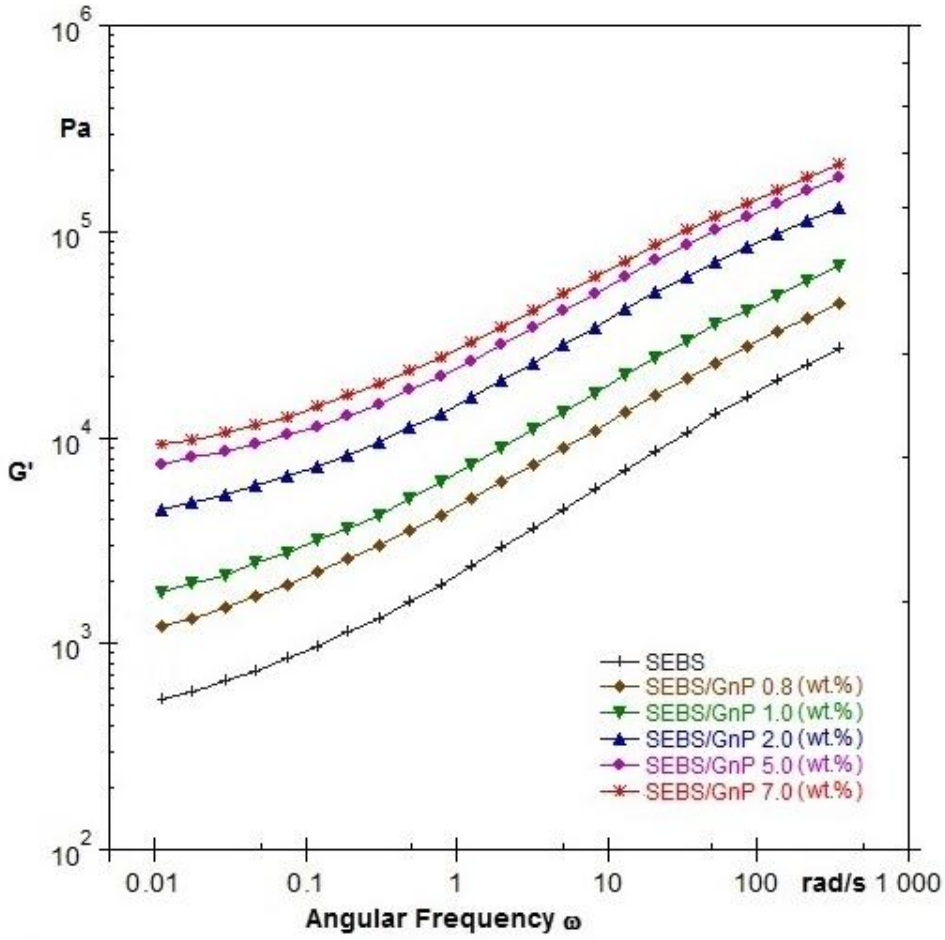

Figure 5. Curves of G' as a function of frequency of neat SEBS and SEBS/GnP nanocomposites at different GnP weight fraction

Table 1. Low frequency slope of log G' vs. log ω for neat SEBS, and SEBS/GnP and SEBS/CNT nanocomposites at different carbon nanoadditive weight fractions

SEBS	Low frequency slope of log G' vs. log ω	SEBS/GnP (wt.%)	Low frequency slope of log G' vs. log ω	SEBS/CNT (wt.%)	Low frequency slope of log G' vs. log ω
0.32		0.8	0.32	0.5	0.26
		1	0.30	0.8	0.22
		2	0.27	1	0.19
		5	0.24	2	0.14
		7	0.24	3	0.11
		-	-	5	0.05

Figure 5 shows that the SEBS used in this work presented a terminal behavior, with a slope of 0.32 (between 1 and 0.01 rad.s^{-1}), as shown in Table 1, which is characteristic of a cylindrical morphology [32]. The figure also indicates that the addition of GnP results in an increase of G' for the whole range of frequencies without a significant decrease in slope of log G' vs. log ω for low frequencies, showing that the GnP acts as a filler, but does not significantly change the relaxation of the SEBS chain; this in turn indicates that it is probably not well dispersed, and does not present a significant interaction with the SEBS matrix.

Nanocomposites of SEBS/CNT were also prepared in order to characterize the difference between the dispersion of the different carbon nanoadditives in the SEBS matrix. Figure 6 shows the rheological behavior (SAOS) of neat SEBS and SEBS/CNT nanocomposites at low frequencies.

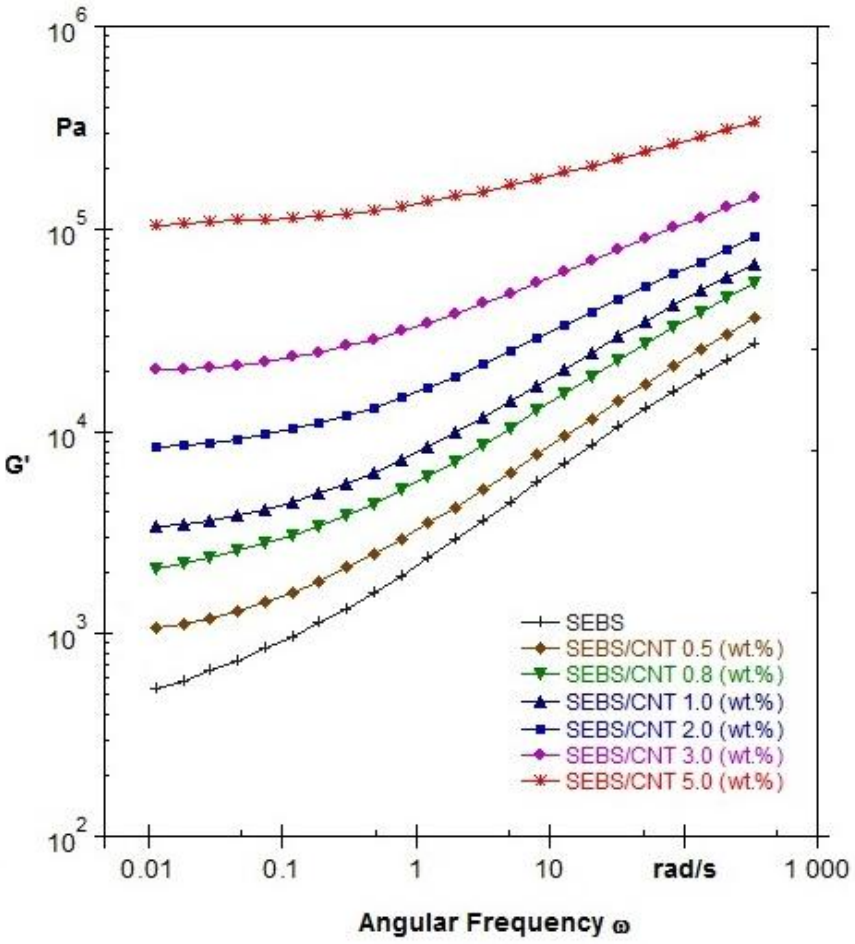

Figure 6. Curves of G' as a function of frequency of neat SEBS and SEBS/CNT nanocomposites at different CNT weight fractions

It can be seen that the addition of CNT results in an increase of G' for the whole range of frequencies, but also in a decrease in slope of log G' vs log ω at low frequencies, indicating that not only does CNT act as a filler; it also reduces the mobility of SEBS chains, most likely due to the formation of a percolating network of nanoparticles [32]. As shown in Figure 6, upon addition of 3.0 to 5.0 wt.% of CNT, almost horizontal non-terminal plateaus were formed in the G' curves, indicating that carbon nanoparticles hinder the low frequency relaxation processes, causing the nanocomposite to become highly solid-like. This behavior is observed for composites where particles are intercalated or exfoliated, and the degree of the effects vary depending on the microstructure and the affinity between the particle and the matrix [32].

Raman spectroscopy was used as a tool to investigate the presence of non-covalent π-π interactions between the carbon nanoparticles and the aromatic rings of polymer chains. Figure 7 shows Raman spectra of the pristine GnP, as well as SEBS/GnP nanocomposites with 10 wt.% of GnP.

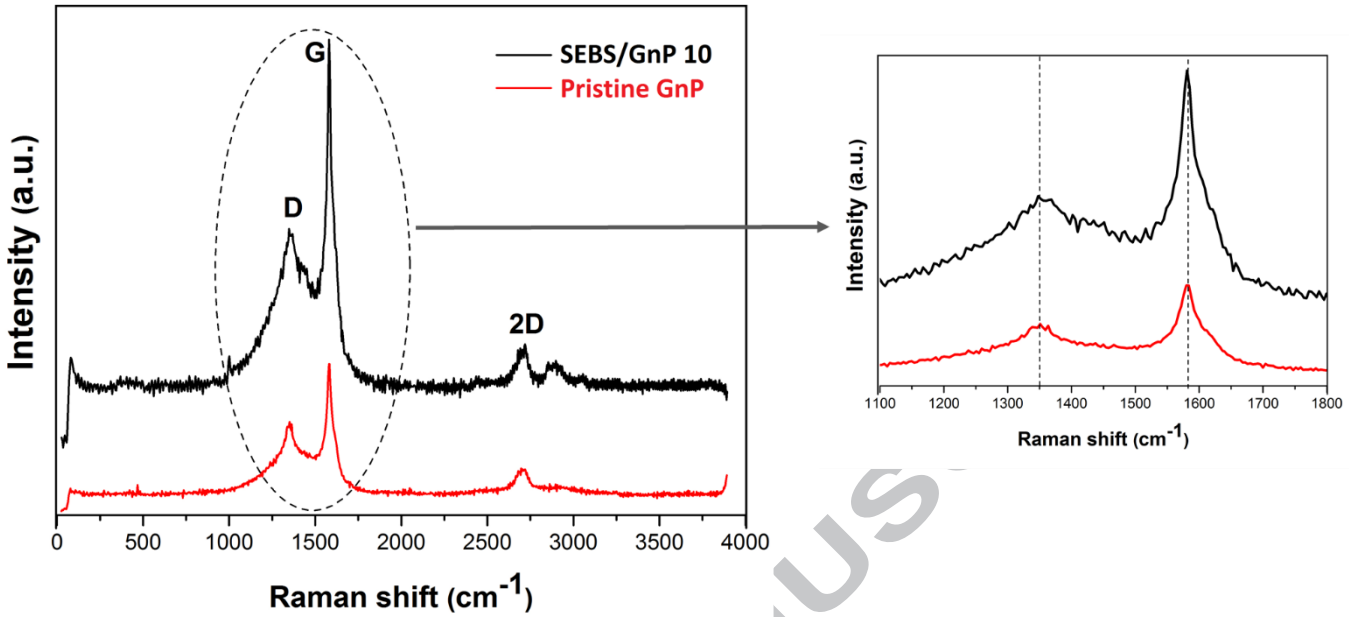

Figure 7. Raman spectra of pristine GnP and SEBS/GnP nanocomposites with 10 wt.% GnP (on the left), and blow-up of the spectra in the 1100-1800 cm^{-1} region (on the right)

The pristine GnP presented the typical D peak (related to the in-plane vibration of sp^2 carbon atoms) and G peak (correlated to defects) [34] at 1363 cm^{-1} and 1580 cm^{-1}, respectively. Compared to the pristine GnP peaks, the spectra of the SEBS/GnP nanocomposite did not present any shift in the D-band and G-band peaks. This result indicates that there is little or no interaction between the polymer matrix and the graphene nanoparticles, which is in agreement with the results exhibited by SAOS analysis.

In a previous work, we showed that the pristine CNT presented the characteristic D peak at 1335 cm^{-1}, and the G peak at 1573 cm^{-1}. When compared to the pristine CNT peaks, the spectra of the SEBS/CNT nanocomposite presented shifts of 12 cm^{-1} (1347 cm^{-1}) and 19 cm^{-1} (1592 cm^{-1}) in the D-band and G-band peaks, respectively [29]. This indicates the existence of non-covalent interfacial interactions between CNT and the polymer matrix [22, 34, 35].

3.2. Electrical conductivity

Figure 8 presents the electrical conductivity of SEBS/GnP as a function of the GnP weight faction. It can be seen that the SEBS/GnP nanocomposites present a nearly constant increase in electrical conductivity with an increase in the GnP content, and do not present a sharp electrical insulating-conductor transition.

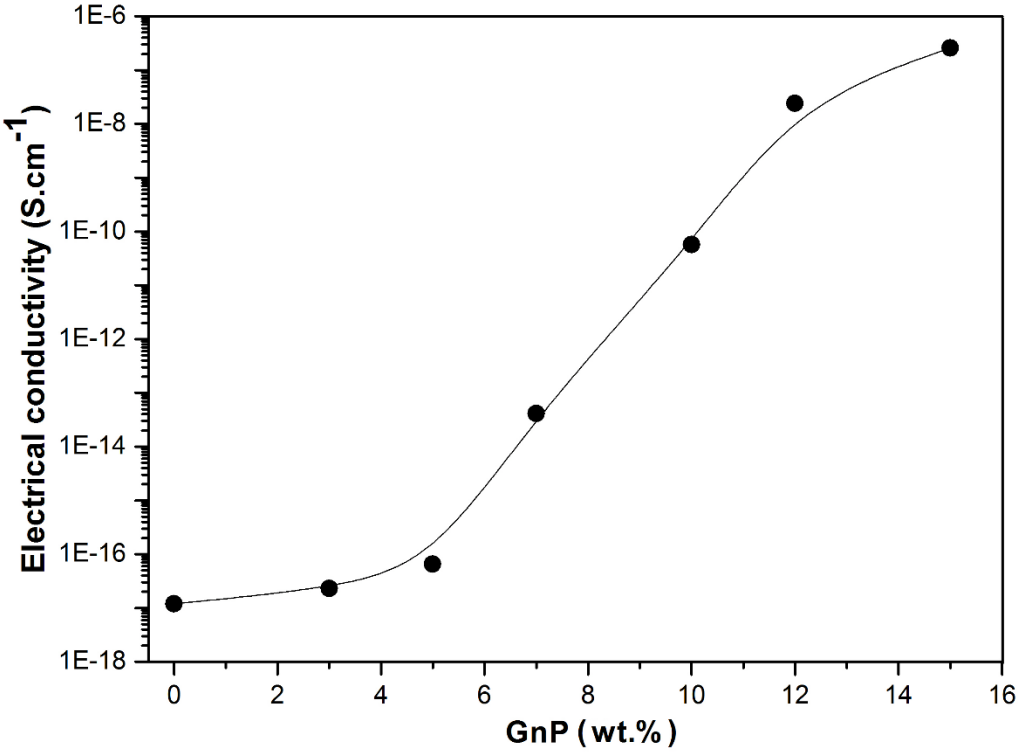

Figure 8. Electrical conductivity of SEBS/GnP nanocomposites at different GnP weight fractions

Results obtained for SEBS/CNT nanocomposites prepared in our prior work, were considerably different. SEBS/CNT presented a sharp electrical insulating-conductor transition, and an electrical conductivity increase of 17 orders of magnitude, reaching ≈1 $S.cm^{-1}$ at 8 wt.% of CNT [29].

For the hybrid nanocomposites prepared in the present work, the electrical conductivity is a function of the CNT content. In other words, hybrid nanocomposites of SEBS/GnP/CNT exhibit electrical conductivities similar to those for SEBS/CNT nanocomposites, for the same weight fraction of CNT, while the weight fraction of graphene does not contribute to enhance the electrical conductivity. This result was expected at some point, considering that the CNT presented better interaction (shown through Raman spectroscopy and rheological analysis) with the SEBS matrix than the graphene nanoplatelets. Table 2 shows a comparison of the electrical conductivity of SEBS/GnP, SEBS/CNT, and SEBS/GnP/CNT nanocomposites.

Table 2. Comparison of the electrical conductivity of SEBS/GnP, SEBS/CNT, and SEBS/GnP/CNT nanocomposites at different weight fractions of carbon nanoadditives

SEBS/GnP (wt.%)	Electrical conductivity ($S.cm^{-1}$)	SEBS/GnP/CNT (wt.%)	Electrical conductivity ($S.cm^{-1}$)	SEBS/CNT [29] (wt.%)	Electrical conductivity [29] ($S.cm^{-1}$)
0	1.2E-17	0	1.2E-17	0	1.2E-17
3	2.3E-17	7/3	3.8E-1	3	1.1E-1
5	6.5E-17	5/5	8.4E-1	5	9.4E-01
7	4.1E-14	2/8	1.4	8	1.4
10	5.7E-11	7/8	1.5	10	1.8
15	2.6E-7	5/10	2.7	15	2.2

The maximum electrical conductivity of the SEBS/GnP nanocomposites was 2.6E-7 $S.cm^{-1}$ at 15 wt.% of GnP. For the hybrid nanocomposites, the electrical conductivity remained somewhat constant, between 1.4 and 2.7 $S.cm^{-1}$, for compounds with a CNT equal to or higher than 8 wt.%.

3.3. Electromagnetic shielding effectiveness and dielectric properties

The electromagnetic interference shielding effectiveness (EMI-SE) of the nanocomposites was established using experimental data and equations 3 and 4 [6, 10, 14, 15, 31, 36].

$$\text{EMI SE} = \text{SER} + \text{SEA} = 10\log\frac{I}{I-R} + 10\log\frac{I-R}{T} = 20\log\frac{I}{T} \quad (3)$$

$$I = 1 = R + A + T \quad (4)$$

where SE_R, and SE_A correspond to shielding mechanisms by reflection and absorption, respectively.

Figure 9 shows the EMI-SE of SEBS/GnP nanocomposites at different GnP weight fractions as a function of frequency.

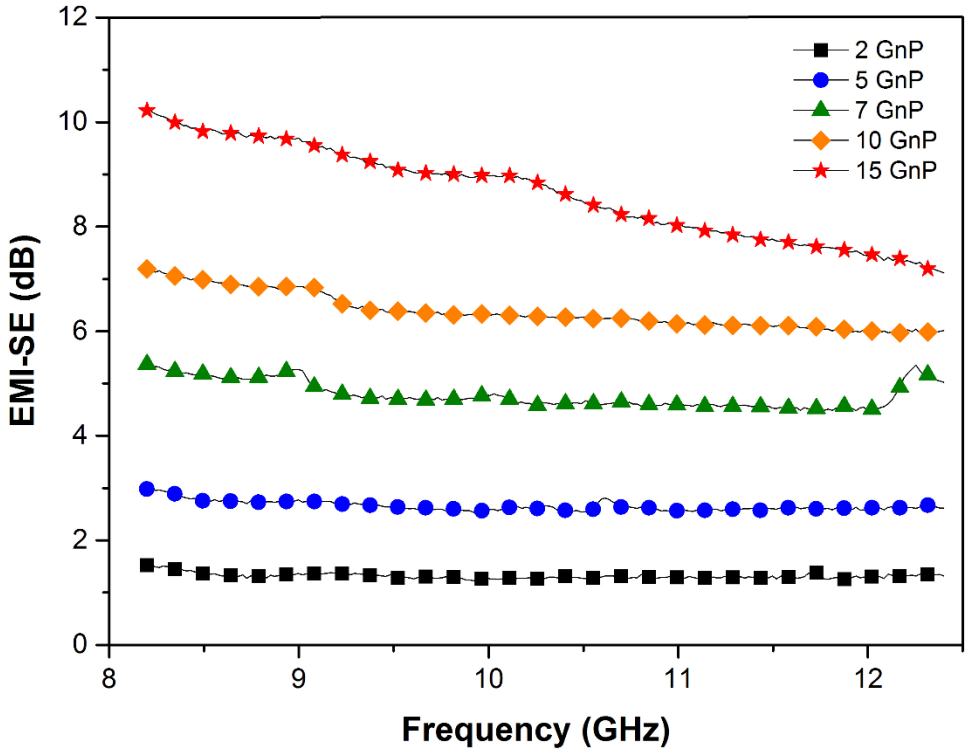

Figure 9. Shielding effectiveness of SEBS/GnP nanocomposites at different GnP weight fractions as a function of frequency

For commercial applications, the minimum EMI-SE required is 20 dB, which represents a 99.00% attenuation of the incident radiation [1, 8, 10-12, 14, 15]. As shown in Figure 9, SEBS/GnP nanocomposites do not satisfy the minimum shielding effectiveness requirement for all the compositions prepared. The EMI-SE for the nanocomposite with 15 wt.% of GnP (maximum weight fraction of nanoadditive used in this work) was 8.63 dB (86.02% attenuation) on average. However, as shown in Figure 10, hybrid nanocomposites of SEBS/GnP/CNT presented much higher EMI-SE.

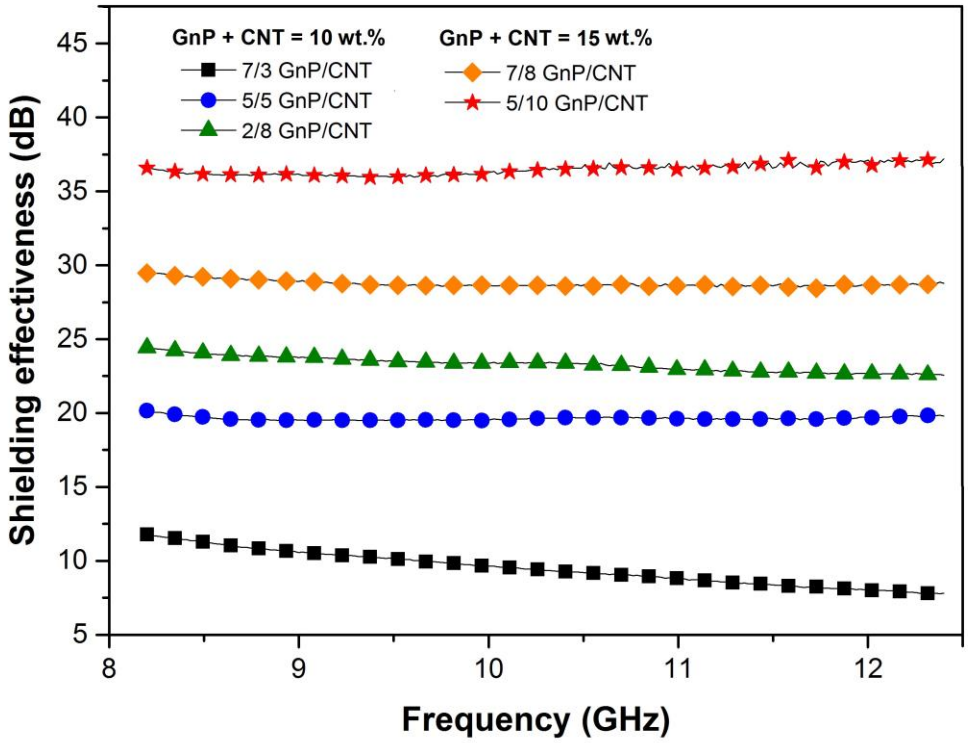

Figure 10. Shielding effectiveness of SEBS/GnP/CNT nanocomposites at different GnP/CNT weight fractions as a function of frequency

At this point, it is important to consider that in a previous work, SEBS/CNT nanocomposites presented satisfactory results for nanocomposites with 10 wt.% (20.78 dB, 99.16% attenuation) and 15 wt.% (30.07 dB, 99.90% attenuation) of CNT [29]. In the present work, we prepared SEBS/GnP/CNT hybrid nanocomposites with a total loading of 10 and 15 wt.%, while varying the amount of the different nanoadditives.

For the SEBS/GnP/CNT nanocomposite at the absolute loading fraction of 10 wt.%, 7/3 wt.% of GnP/CNT, respectively, the EMI-SE was 9.48 dB (88.36% attenuation). This result was higher than the EMI-SE of 10 wt.% of GnP in SEBS/GnP nanocomposites, but still lower than the minimum requirement. However, the increase in CNT weight fractions in the nanocomposites considerably enhanced the EMI-SE. For the SEBS/GnP/CNT nanocomposite with 5/5 wt.% of GnP/CNT, the EMI-SE was 19.63 dB (98.91% attenuation). Lastly, for the nanocomposites with a minimum CNT loading equal to or higher than 8 wt.%, the shielding effectiveness value requirement was satisfied. Table 3 summarizes the EMI-SE results for the different compositions.

Table 3. Shielding effectiveness (dB) and percentage of attenuated radiation of SEBS/GnP, SEBS/CNT, and SEBS/GnP/CNT nanocomposites at different carbon nanoadditive weight fractions (the light gray highlights correspond to 10 wt.% of absolute carbon nanoadditive loading fraction, while the dark gray ones correspond to 15 wt.% of absolute carbon nanoadditive loading fraction)

SEBS/GnP (GnP wt.%)	EMI-SE (dB)	Radiation attenuated (%)	SEBS/CNT (CNT wt.%) [29]	EMI-SE (dB) [29]	Radiation attenuated (%) [29]	Total loading (GnP+CNT)	SEBS/GnP /CNT (GnP /CNT wt.%)	EMI-SE (dB)	Radiation attenuated (%)
2	1.32	26.16	3	6.88	79.42	10 wt.%	7/3	9.48	88.36
5	2.66	45.74	5	10.67	91.30		5/5	19.63	98.91
7	4.78	66.68	8	17.02	98.01		2/8	23.30	99.53
10	6.37	76.88	10	20.78	99.16	15 wt.%	7/8	28.76	99.87
15	8.63	86.02	15	30.07	99.90		5/10	36.47	99.98

For the SEBS/GnP/CNT nanocomposite with a total of 10 wt.% of carbon nanoadditives, in a portion of 2/8 wt.% of GnP/CNT, respectively, the EMI-SE was 23.30 dB (99.53% attenuation). This result was much higher than the EMI-SE of SEBS/GnP and SEBS/CNT nanocomposites at the same absolute loading fraction. Further, the EMI-SE was higher than the sum of the EMI-SE of SEBS/GnP with 2 wt.% of GnP and SEBS/CNT with 8 wt.% of CNT. These results show a synergic effect between the CNT and GnP regarding shielding effectiveness. A similar behavior was observed for the hybrid nanocomposites with higher weight fractions of carbon nanoadditives where the CNT >> GnP.

For the hybrid nanocomposite with an absolute carbon nanoadditive loading fraction of 15 wt.%, in a portion of 7/8 wt.% of GnP/CNT, the EMI-SE was 28.76 dB (99.87% attenuation). Finally, the higher EMI-SE of 36.47dB (99.98% attenuation) was achieved in the SEBS/GnP/CNT nanocomposite with 5/10 wt.% of GnP/CNT. Again, the EMI-SE was much higher than the effectiveness of the single nanocomposites at the same total loading fraction, i.e., greater than the sum of the EMI-SE of SEBS/GnP with 5 wt.% of GnP and SEBS/CNT with 10 wt.% of CNT, and the synergic effect was confirmed once again.

According to the literature, the advantage of preparing hybrid nanocomposites for electromagnetic shielding applications is the improvement of the conductive network due to the combination of carbon nanoadditives of different shapes, which may result in the synergic effects on the EMI-SE [6, 11, 13]. Sharma, S. K. et al. prepared hybrid nanocomposites of acrylonitrile butadiene styrene (ABS), CNT, and GR by dry tumble mixing followed by hot compaction. They showed that the EMI-SE of the nanocomposites increased from 7.5 to 26.8 dB with the addition of 1 wt.% of CNT to an ABS/GR nanocomposite, resulting in a synergic effect on the EMI-SE in the hybrid nanocomposite. According to the authors, the synergism was due to an improvement of the connectivity of the conductive network by the combination of the two different carbon nanoadditives [6]. Maiti, S., et al. prepared hybrid nanocomposites of polystyrene (PS), CNT, and graphite nanoplates by in situ polymerization. With a portion of 2/1.5 wt.% of CNT/Graphite nanoplate, respectively, the commercially applicable EMI-SE (≈ 20.2 dB) was achieved. The authors state that the suitable EMI-SE with low amounts of nanoadditives was achieved due to the strong π-π interactions between PS and the carbon additives during in situ polymerization, and because of the

interconnected conductive network formed [10]. Al-Saleh, M. H., and Saadeh, W. H. obtained nanocomposites of ABS, CNT, and carbon black (CB) by solution casting followed by hot compression. Although the hybrid nanocomposites did not present synergic effects, the authors showed that small quantities of CNT could be replaced by CB, decreasing the final cost of the nanocomposites, without impairing the EMI-SE [11].

In EMI shielding materials, the capacity to attenuate the incident electromagnetic radiation is the sum of the different shielding mechanisms, according the Equation 3. Thus, in order to assess the intrinsic attenuation capacity of the nanocomposites via different mechanisms, the impact of reflection (SE_R) and absorption (SE_A) mechanisms on the total shielding effectiveness was also evaluated. Table 4 shows the total EMI-SE, SE_R, and SE_A of the SEBS/GnP and SEBS/GnP/CNT nanocomposites at different carbon nanoadditive weight fractions.

Table 4. Shielding effectiveness (dB), SE_R, and SE_A of the SEBS/GnP, SEBS/CNT, and SEBS/GnP/CNT nanocomposites at different carbon nanoadditive weight fractions

SEBS/GnP (GnP wt.%)	EMI-SE (dB)	SE_R	SE_A	SEBS/CNT (CNT wt.%) [29]	EMI-SE (dB) [29]	SE_R	SE_A	Total loading (GnP +CNT)	SEBS/GnP/CNT (GnP/CNT wt.%)	EMI-SE (dB)	SE_R	SE_A
2	1.32	1.18	0.14	3	6.88	4.46	2.42	10 wt.%	7/3	9.48	5.08	4.40
5	2.66	2.39	0.27	5	10.67	4.44	6.23		5/5	19.63	4.61	15.02
7	4.78	4.43	0.35	8	17.02	3.79	13.23		2/8	23.30	5.39	17.91
10	6.37	5.94	0.43	10	20.78	4.75	16.03	15 wt.%	7/8	28.76	6.37	22.39
15	8.63	7.09	1.54	15	30.07	5.21	24.86		5/10	36.47	6.90	29.57

For all the SEBS/GnP nanocomposites prepared in the present work, the $SE_R > SE_A$. However, for the hybrid SEBS/GnP/CNT nanocomposites, the contribution by the SE_A mechanism is proportionally enhanced with increased CNT loading. More specifically, for the nanocomposite with 7/3 wt.% of GnP/CNT, $SE_R > SE_A$, while for all the other SEBS/GnP/CNT nanocomposites, $SE_A > SE_R$. These results were expected, since it is known that the SE_A increases as the nanocomposite's electrical conductivity is increased and/or with a narrower space between the carbon nanoparticles. However, unlike with single-component materials, an increase in SE_A for composite materials is non-linear, and to date, no theoretical interpretation has been established for the correlation between EMI-SE, conductive additive connectivity, electrical conductivity, and electrical permittivity specifically for composites [36].

The complex permittivity is a useful parameter for analyzing the EMI-SE of polymeric nanocomposites based on carbon nanoparticles [7-9]. According to [8, 14, 37, 38], in polymer nanocomposites, the real permittivity (ε') (polarization) depends on the number of micro-capacitors and the polarization centers formed inside the material; here, polarization centers result from defects in the nanoadditive structure, while micro-capacitors are the carbon nanoparticles or their aggregates acting as electrodes in the insulating polymer matrix. On the other hand, the imaginary permittivity (ε") (dielectric loss) is related to the dissipation of energy due to the conductive paths formed inside the nanocomposite.

Figure 11 shows ε' and ε" as a function of frequency in the 8.2 - 12.4 GHz range for the a), b), SEBS/GnP and c), d), SEBS/GnP nanocomposites, respectively, at different weight fractions of carbon nanoadditives.

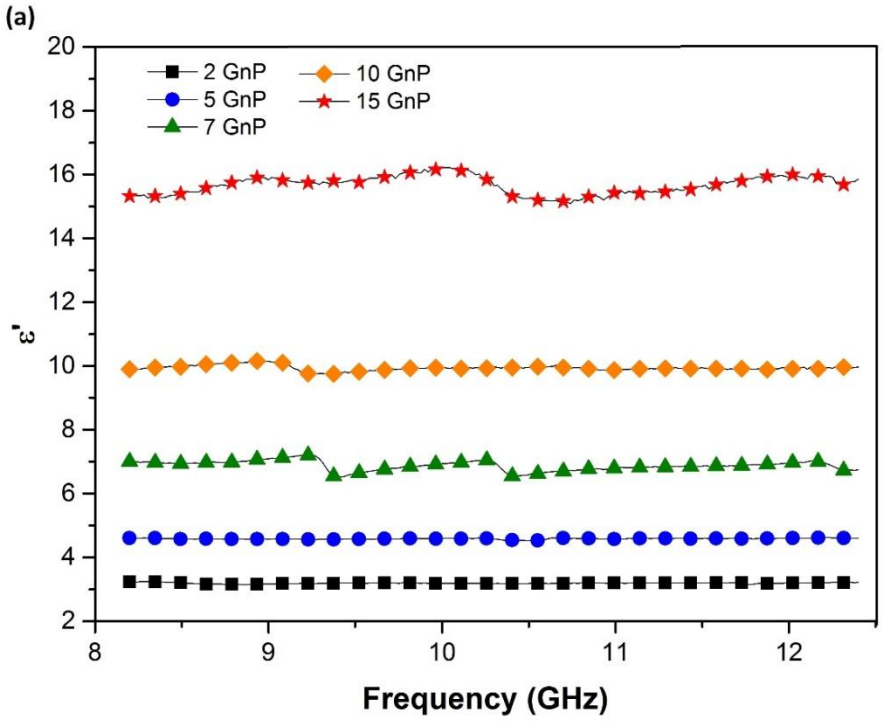
(a)
2 GnP
5 GnP
7 GnP
10 GnP
15 GnP
ε'
Frequency (GHz)

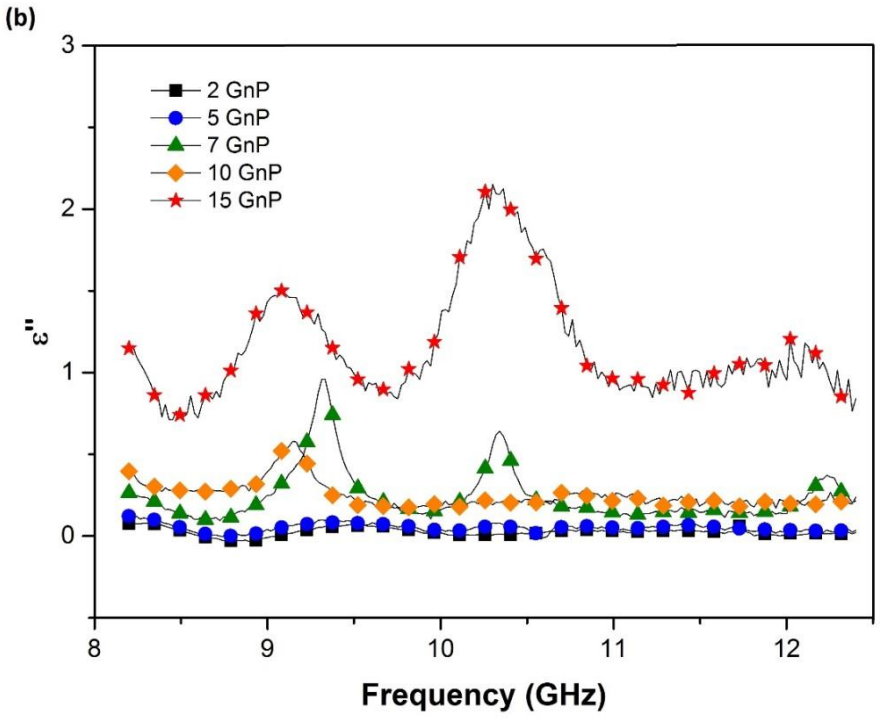
(b)
2 GnP
5 GnP
7 GnP
10 GnP
15 GnP
ε''
Frequency (GHz)

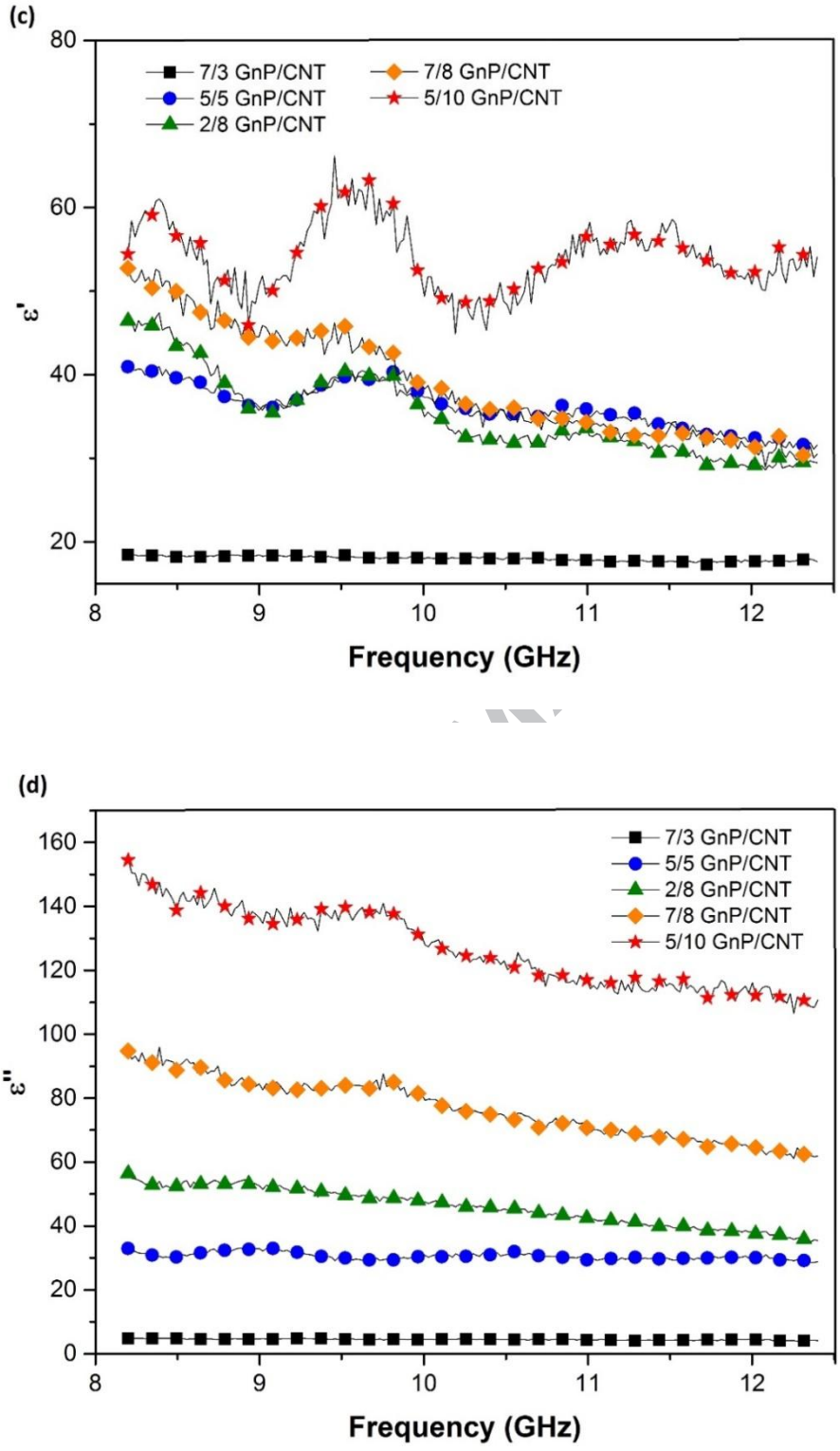

Figure 11. a) c) Real (ε') and b) d) imaginary (ε") permittivity versus frequency of SEBS/GnP and SEBS/GnP/CNT nanocomposites, respectively, at different carbon nanoadditive weight fractions

For all the samples, ε' and ε" were enhanced as the weight fractions of carbon nanoadditives were increased in the nanocomposites. Increases in ε' with higher carbon nanoadditive loadings are expected since the number of structural defects and micro-capacitors inside the nanocomposites is also higher. Further, with higher amounts of carbon nanoadditives, the gap between the nanoparticles decreases, increasing the polarization inside the material. Higher values of ε" are also expected for nanocomposites with higher carbon nanoadditive loadings due to the higher amount of conductive paths inside the nanocomposites.

For all the SEBS/GnP nanocomposites, ε' > ε". However, the hybrid nanocomposites presented a different behavior. For the nanocomposite with 7/3 wt.% of GnP/CNT (with a total of 10 wt.% of carbon nanoadditives), ε' > ε", while for the compound of 5/5 wt.% of GnP/CNT (with a total of 10 wt.% of carbon nanoadditives), ε' ≈ ε", and for the nanocomposites with higher CNT loading, ε' < ε", which means that at this point, the energy dissipation is more effective because of the higher number of paths forming the conductive network throughout the nanocomposite. These results justify the higher EMI-SE of the hybrid nanocomposites with CNT content higher than 8 wt.%.

4. CONCLUSIONS

Hybrid nanocomposites of SEBS/GnP/CNT prepared by melt compounding exhibited high electrical conductivity, as well as EMI-SE suitable for commercial applications. The electrical conductivity increased by 17 orders of magnitude when compared to that of pure matrix, reaching 1.4 $S.cm^{-1}$ at 2/8 wt.% of GnP/CNT (with a total of 10 wt.% of carbon nanoadditives). For the hybrid nanocomposites with CNT loading equal to or higher than 8 wt.%, the conductivity leveled off. The EMI-SE of the SEBS/GnP/CNT nanocomposite at the absolute loading fraction of 10 wt.% of carbon nanoadditives, in a portion of 2/8 wt.% of GnP/CNT, was 23.30 dB (99.53% attenuation). For the hybrid nanocomposite with a total of 15 wt.%, in a GnP/CNT fraction of 5/10 wt.%, the EMI-SE was 36.47dB (99.98% attenuation). These results confirm the synergic effect between the CNT and GnP regarding shielding effectiveness for the nanocomposites for which CNT >> GnP, since the EMI-SE of the hybrid nanocomposites of SEBS/GnP/CNT was higher than the sum of the EMI-SE of the single nanocomposites of SEBS/GnP and SEBS/CNT. SEBS/GnP nanocomposites presented much lower electrical conductivity and EMI-SE than did the hybrid nanocomposites. The maximum electrical conductivity achieved with 15 wt.% of GnP was 2.6E-7 $S.cm^{-1}$, and the maximum EMI-SE was 8.63 dB. For all samples, ε' and ε" were enhanced as the weight fractions of carbon nanoadditives were increased in the nanocomposites. For all SEBS/GnP nanocomposites, ε' > ε". However, for the hybrid nanocomposite with 7/3 wt.% of GnP/CNT (with a total of 10 wt.% of carbon nanoadditives), ε' > ε"; for the 5/5 wt.% (with a total of 10 wt.% of carbon nanoadditives), ε' ≈ ε"; and for the nanocomposites with higher CNT loading, ε' < ε". These results justify the higher EMI-SE of the hybrid nanocomposites with CNT loadings higher than 8 wt.%., which is probably due to the higher number of paths in the conductive network throughout the nanocomposites, which resulted in an increase in energy dissipation. By FEG-SEM, GnP exhibited a non-homogeneous morphology, showing to be a mixture of multi-walled graphene and expanded graphite. CNT presented the characteristic morphology of MWCNT. Both carbon nanoparticles presented decent distributions

throughout the matrix, as well as good adhesion due to the absence of significant voids. Rheological analyses showed that CNT could be properly dispersed into the SEBS matrix. On the other hand, it was not possible to properly disperse GnP in the matrix by melt compounding with the processing parameters used in this work. Raman spectroscopy and rheological analyses showed that SEBS/GnP nanocomposites did not present interactions with the SEBS matrix. The morphological characterization suggests that the higher electrical conductivity and EMI-SE results for the hybrid nanocomposites when compared to the SEBS/GnP nanocomposites are due to the better dispersion and higher interactions of CNT with the matrix, versus the GnP.

Acknowledgements

The authors gratefully acknowledge the financial support of the Natural Sciences and Engineering Research Council of Canada (NSERC), Conselho Nacional de Desenvolvimento Científico e Tecnológico (CNPq), Coordenação de Aperfeiçoamento de Pessoal de Ensino Superior (CAPES), and Fundação de Amparo à Pesquisa e Inovação do Estado de Santa Catarina (FAPESC). We are also truly grateful to the Central Electron Microscopy Laboratory, Santa Catarina Federal University (LCME-UFSC), for the FEG-SEM analysis.

REFERENCES

1. Maiti, S. and B.B. Khatua, *Graphene nanoplate and multiwall carbon nanotube–embedded polycarbonate hybrid composites: High electromagnetic interference shielding with low percolation threshold.* Polymer Composites, 2016. **37**(7): p. 2058-2069.
2. Calisi, N., et al., *Factors affecting the dispersion of MWCNTs in electrically conducting SEBS nanocomposites.* European Polymer Journal, 2013. **49**(6): p. 1471-1478.
3. Xiong, Y., et al., *Reduced graphene oxide/hydroxylated styrene–butadiene–styrene tri-block copolymer electroconductive nanocomposites: Preparation and properties.* Materials Science and Engineering: B, 2012. **177**(14): p. 1163-1169.
4. Das, T.K. and S. Prusty, *Graphene-Based Polymer Composites and Their Applications.* Polymer-Plastics Technology and Engineering, 2013. **52**(4): p. 319-331.
5. Kuilla, T., et al., *Recent advances in graphene based polymer composites.* Progress in Polymer Science, 2010. **35**(11): p. 1350-1375.
6. Sharma, S.K., et al., *Synergic effect of graphene and MWCNT fillers on electromagnetic shielding properties of graphene-MWCNT/ABS nanocomposites.* RSC Advances, 2016. **6**(22): p. 18257-18265.
7. Micheli, D., et al., *X-Band microwave characterization of carbon-based nanocomposite material, absorption capability comparison and RAS design simulation.* Composites Science and Technology, 2010. **70**(2): p. 400-409.
8. Cao, M.-S., et al., *Ultrathin graphene: electrical properties and highly efficient electromagnetic interference shielding.* Journal of Materials Chemistry C, 2015. **3**(26): p. 6589-6599.
9. Aloia, A.G.D., et al. *Synthesis and characterization of graphene-based nanocomposites for EM shielding applications*. in *Electromagnetic Compatibility (EMC EUROPE), 2013 International Symposium on*. 2013.

10. Maiti, S., et al., *Polystyrene/MWCNT/Graphite Nanoplate Nanocomposites: Efficient Electromagnetic Interference Shielding Material through Graphite Nanoplate–MWCNT–Graphite Nanoplate Networking.* ACS Applied Materials & Interfaces, 2013. **5**(11): p. 4712-4724.
11. Al-Saleh, M.H. and W.H. Saadeh, *Hybrids of conductive polymer nanocomposites.* Materials & Design, 2013. **52**: p. 1071-1076.
12. Kim, M.-S., et al., *Synergistic effects of carbon nanotubes and exfoliated graphite nanoplatelets for electromagnetic interference shielding and soundproofing.* Journal of Applied Polymer Science, 2013. **130**(6): p. 3947-3951.
13. Lin, J.-H., et al., *Improvement in Mechanical Properties and Electromagnetic Interference Shielding Effectiveness of PVA-Based Composites: Synergistic Effect Between Graphene Nano-Sheets and Multi-Walled Carbon Nanotubes.* Macromolecular Materials and Engineering, 2016. **301**(2): p. 199-211.
14. Al-Saleh, M.H., W.H. Saadeh, and U. Sundararaj, *EMI shielding effectiveness of carbon based nanostructured polymeric materials: A comparative study.* Carbon, 2013. **60**(0): p. 146-156.
15. Jia, L.-C., et al., *Electrically conductive and electromagnetic interference shielding of polyethylene composites with devisable carbon nanotube networks.* Journal of Materials Chemistry C, 2015. **3**(36): p. 9369-9378.
16. Wang, D., et al., *Characterization of morphology and mechanical properties of block copolymers using atomic force microscopy: Effects of processing conditions.* Polymer, 2012. **53**(9): p. 1960-1965.
17. Rath, T. and Y. Li, *Nanocomposites based on polystyrene-b-poly(ethylene-r-butylene)-b-polystyrene and exfoliated graphite nanoplates: Effect of nanoplatelet loading on morphology and mechanical properties.* Composites Part A: Applied Science and Manufacturing, 2011. **42**(12): p. 1995-2002.
18. Li, Y. and H. Shimizu, *Toward a Stretchable, Elastic, and Electrically Conductive Nanocomposite: Morphology and Properties of Poly[styrene-b-(ethylene-co-butylene)-b-styrene]/Multiwalled Carbon Nanotube Composites Fabricated by High-Shear Processing.* Macromolecules, 2009. **42**(7): p. 2587-2593.
19. Meier, J.G., et al., *Processing dependency of percolation threshold of MWCNTs in a thermoplastic elastomeric block copolymer.* Polymer, 2011. **52**(8): p. 1788-1796.
20. Carastan, D.J., et al., *Morphological evolution of oriented clay-containing block copolymer nanocomposites under elongational flow.* European Polymer Journal, 2013. **49**(6): p. 1391-1405.
21. Helal, E., et al., *Styrenic block copolymer-based nanocomposites: Implications of nanostructuration and nanofiller tailored dispersion on the dielectric properties.* Polymer, 2015. **64**: p. 139-152.
22. Vasileiou, A.A., et al., *The role of non-covalent interactions and matrix viscosity on the dispersion and properties of LLDPE/MWCNT nanocomposites.* Polymer, 2013. **54**(19): p. 5230-5240.
23. Liu, Y.-T., X.-M. Xie, and X.-Y. Ye, *High-concentration organic solutions of poly(styrene-co-butadiene-co-styrene)-modified graphene sheets exfoliated from graphite.* Carbon, 2011. **49**(11): p. 3529-3537.
24. Spitalsky, Z., et al., *Carbon nanotube–polymer composites: Chemistry, processing, mechanical and electrical properties.* Progress in Polymer Science, 2010. **35**(3): p. 357-401.

25. Tsuyohiko, F. and N. Naotoshi, *Non-covalent polymer wrapping of carbon nanotubes and the role of wrapped polymers as functional dispersants.* Science and Technology of Advanced Materials, 2015. **16**(2): p. 024802.
26. Pöllänen, M., et al., *Influence of carbon nanotube–polymeric compatibilizer masterbatches on morphological, thermal, mechanical, and tribological properties of polyethylene.* Composites Science and Technology, 2011. **71**(10): p. 1353-1360.
27. Bilalis, P., et al., *Non-covalent functionalization of carbon nanotubes with polymers.* RSC Advances, 2014. **4**(6): p. 2911-2934.
28. Thomassin, J.-M., et al., *Functionalized polypropylenes as efficient dispersing agents for carbon nanotubes in a polypropylene matrix; application to electromagnetic interference (EMI) absorber materials.* Polymer, 2010. **51**(1): p. 115-121.
29. Kuester, S., et al., *Electromagnetic interference shielding and electrical properties of nanocomposites based on poly (styrene-b-ethylene-ran-butylene-b-styrene) and carbon nanotubes.* European Polymer Journal, 2016. **77**: p. 43-53.
30. Saini, P. and M. Arora, *Microwave Absorption and EMI Shielding Behavior of Nanocomposites Based on Intrinsically Conducting Polymers, Graphene and Carbon Nanotubes.* New Polymers for Special Applications, 2012: p. 71-112.
31. Ramôa, S.D.A.S., et al., *Electrical, rheological and electromagnetic interference shielding properties of thermoplastic polyurethane/carbon nanotube composites.* Polymer International, 2013. **62**(10): p. 1477-1484.
32. Carastan, D.J., et al., *Linear viscoelasticity of styrenic block copolymers–clay nanocomposites.* Rheologica Acta, 2008. **47**(5): p. 521-536.
33. Demarquette, N.R., Carastan, D., *Rheological Behavior of Nanocomposites*.
34. Zhao, L., et al., *Reactive bonding mediated high mass loading of individualized single-walled carbon nanotubes in an elastomeric polymer.* Nanoscale, 2012. **4**(20): p. 6613-6621.
35. Linton, D., et al., *The importance of chain connectivity in the formation of non-covalent interactions between polymers and single-walled carbon nanotubes and its impact on dispersion.* Soft Matter, 2010. **6**(12): p. 2801-2814.
36. Al-Saleh, M.H. and U. Sundararaj, *Electromagnetic interference shielding mechanisms of CNT/polymer composites.* Carbon, 2009. **47**(7): p. 1738-1746.
37. Arjmand, M., et al., *Comparative study of electromagnetic interference shielding properties of injection molded versus compression molded multi-walled carbon nanotube/polystyrene composites.* Carbon, 2012. **50**(14): p. 5126-5134.
38. Theilmann, P., et al., *Superior electromagnetic interference shielding and dielectric properties of carbon nanotube composites through the use of high aspect ratio CNTs and three-roll milling.* Organic Electronics, 2013. **14**(6): p. 1531-1537.

HYBRID NANOCOMPOSITES OF THERMOPLASTIC ELASTOMER AND CARBON NANOADDITIVES FOR ELECTROMAGNETIC SHIELDING

Scheyla Kuester, Nicole R. Demarquette, José Carlos Ferreira Jr., Bluma G. Soares, Guilherme M. O. Barra

- Hybrid nanocomposites of SEBS/GnP/CNT were prepared by melt compounding.
- The electrical conductivity was enhanced by 17 orders of magnitude.
- The higher EMI-SE was 36.47dB (99.98% attenuation) achieved in the SEBS/GnP/CNT nanocomposite with 5/10 wt.% of GnP/CNT.
- Results confirm synergic effect between GnP and CNT regarding shielding effectiveness for the nanocomposites for which CNT >> GnP, since the EMI-SE of the hybrid nanocomposites of SEBS/GnP/CNT was higher than the sum of the EMI-SE of the single nanocomposites of SEBS/GnP and SEBS/CNT.

HYBRID NANOCOMPOSITES OF THERMOPLASTIC ELASTOMER AND CARBON NANOADDITIVES FOR ELECTROMAGNETIC SHIELDING

Scheyla Kuester, Nicole R. Demarquette, José Carlos Ferreira Jr., Bluma G. Soares, Guilherme M. O. Barra